Sister chromatids separate during anaphase in a three-stage program as directed by interaxis bridges

Lingluo Chu[a], Zheng Zhang[a,b], Maria Mukhina[a], Denise Zickler[c], and Nancy Kleckner[a,1]

[a]Department of Molecular and Cellular Biology, Harvard University, Cambridge, MA 02138; [b]Chinese Academy of Sciences Key Laboratory of Quantitative Engineering Biology, Shenzhen Institute of Synthetic Biology, Shenzhen Institutes of Advanced Technology, Chinese Academy of Sciences, Shenzhen, 518055, People's Republic of China; and [c]Institute for Integrative Biology of the Cell (I2BC), CNRS, University Paris-Saclay, 91190 Gif-sur-Yvette, France

Contributed by Nancy Kleckner; received December 27, 2021; accepted January 21, 2022; reviewed by Job Dekker and Kazuhiro Maeshima

During mitosis, from late prophase onward, sister chromatids are connected along their entire lengths by axis-linking chromatin/structure bridges. During prometaphase/metaphase, these bridges ensure that sister chromatids retain a parallel, paranemic relationship, without helical coiling, as they undergo compaction. Bridges must then be removed during anaphase. Motivated by these findings, the present study has further investigated the process of anaphase sister separation. Morphological and functional analyses of mammalian mitoses reveal a three-stage pathway in which interaxis bridges play a prominent role. First, sister chromatid axes globally separate in parallel along their lengths, with concomitant bridge elongation, due to intersister chromatin pushing forces. Sister chromatids then peel apart progressively from a centromere to telomere region(s), step-by-step. During this stage, poleward spindle forces dramatically elongate centromere-proximal bridges, which are then removed by a topoisomerase IIα–dependent step. Finally, in telomere regions, widely separated chromatids remain invisibly linked, presumably by catenation, with final separation during anaphase B. During this stage increased separation of poles and/or chromatin compaction appear to be the driving force(s). Cohesin cleavage licenses these events, likely by allowing bridges to respond to imposed forces. We propose that bridges are not simply removed during anaphase but, in addition, play an active role in ensuring smooth and synchronous microtubule-mediated sister separation. Bridges would thereby be the topological gatekeepers of sister chromatid relationships throughout all stages of mitosis.

mitosis | anaphase | interaxis bridges | TopoII decatenation | cohesin

A critical event for eukaryotic cells is the correct segregation of sister chromatids to opposite spindle poles (anaphase) during mitosis. The cytoskeleton components and mechanisms involved in chromosome movement during this process, including separation of sister chromatid centromere/kinetochore regions, have been extensively studied. However, less attention has been paid to the mechanisms that govern separation of sister chromatids along their lengths. It was long considered that connections between sister chromatids along their arms comprise peripheral chromatin connections involving a small amount of cohesin located at the sister/sister interface (1, 2) plus topological catenations (3–5). However, our recent study has revealed that sister chromatids are linked by robust, evenly spaced bridges (6). More specifically, at metaphase, each chromatid comprises a linear array of chromatin loops that emanate from a complex structural axis meshwork. Bridges between sister chromatids link their respective axes and are, themselves "miniature axes" (6) (Fig. 1*A*). Bridges comprise many/all of the same components as the axes themselves, e.g., chromatin, condensin I and II, SMC5/6, and topoisomerase IIα (TopIIα). In addition, bridges have two unique components. First, they contain a small amount of residual cohesin (in addition to the larger amount present at centromeres) corresponding to that detected previously at the intersister interface by lower resolution studies (Fig. 1*A*). Second, they represent positions at which DNA from sister chromatids come together across the interaxis space (6). This feature raises the possibility that bridges might be built upon catenations between loops of sister chromatids (Fig. 1*B*).

Interaxis bridges emerge concomitant with sister chromatid individualization at late prophase and then remain present through metaphase and into anaphase (6). During prometaphase/metaphase, bridges ensure that sister chromatids remain in a parallel, paranemic relationship, without helical coiling, and despite ongoing chromosome turbulence, throughout the compaction process (6, 7). Thereafter, however, in order for sister chromatids to separate at anaphase, these bridges must be removed.

To further understand the nature of this removal process, and its possible functional significance, we examined anaphase sister separation by live cell fluorescence imaging of mammalian chromosomes at high resolution in three-dimensional (3D) space and time. This approach reveals a three-stage bridge-mediated progression, licensed by release of cohesin from bridges, driven by three different types of intersister separation forces, and finalized by TopIIα-mediated processes, likely including TopIIα turnover as well as decatenation. The observed patterns raise the possibility that bridges are active mediators of anaphase sister separation and are thereby the topological gatekeepers of sister chromatids, not only during chromosome compaction as previously shown, but also during anaphase, and thus throughout mitosis.

Significance

A central feature of mitosis is segregation of sister chromatids to opposite poles during anaphase. Our recent work revealed that sister chromatids are linked by robust structural bridges built on topological sister/sister catenations. This unexpected finding implies that separation of sister chromatids is more complex than previously thought. The present study reveals that bridges are removed in a highly programmed three-stage process, all licensed by anaphase onset and cohesin removal, and all promoted by distinct types of intersister separation forces. Removal of bridge-associated cohesin and topoisomerase II–mediated decatenation plays a central role. These findings raise the possibility that the presence and programmed removal of bridges are required for smooth, synchronous, and regular movement of sisters to opposite poles.

Author contributions: L.C. and N.K. designed research; L.C. performed research; L.C. contributed new reagents/analytic tools; L.C., Z.Z., M.M., D.Z., and N.K. analyzed data; and L.C., Z.Z., M.M., D.Z., and N.K. wrote the paper.

Reviewers: J.D., University of Massachusetts Medical School; and K.M., Kokuritsu Idengaku Kenkyujo.

The authors declare no competing interest.

[1]To whom correspondence may be addressed. Email: kleckner@fas.harvard.edu.

This article contains supporting information online at http://www.pnas.org/lookup/suppl/doi:10.1073/pnas.2123363119/-/DCSupplemental.

Published March 2, 2022.

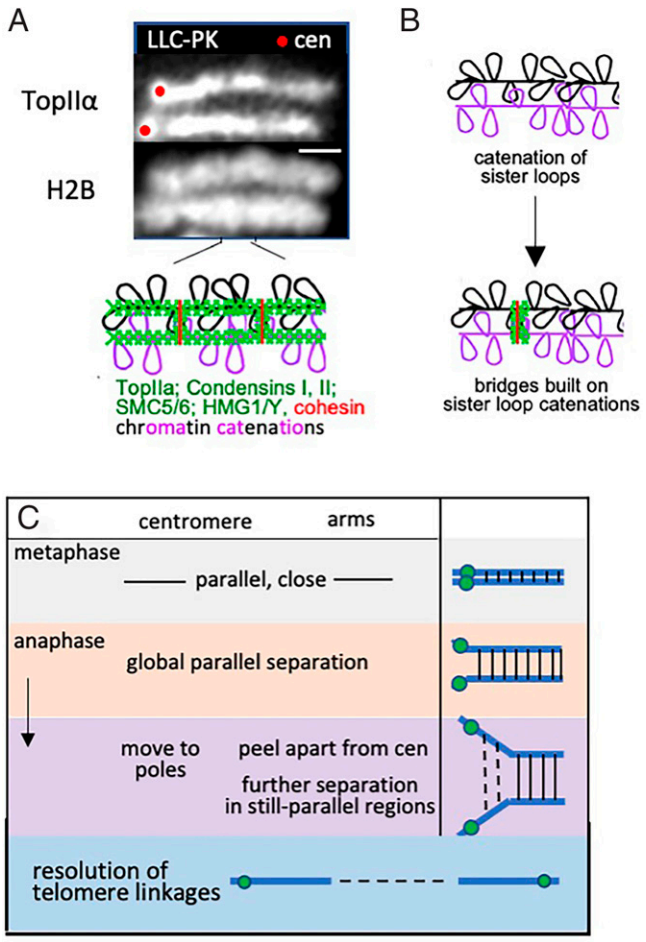

Fig. 1. Sister chromatids are linked by interaxis bridges until the end of anaphase. (*A*) Structure of metaphase chromosomes: Axes (green), loops (black and purple), and interaxis bridges with cohesin (red lines). (*B*) Bridges are built on catenations between sister chromatids. (*C*) Three morphological stages of sister chromatid separation. From *Top* to *Bottom*: From close association at metaphase, sister chromatids undergo: global separation with modest bridge elongation; peeling apart with dramatic bridge extension at separation forks followed by bridge disappearance; and finally delayed bridge removal at telomeres. (*A*, *Bottom* and *B* are adapted from ref. 6). (Scale bars: 1 μm.).

Results

Part I. Anaphase Sister Chromatid Separation Occurs in Three Successive Stages.

Sister chromatid axes separate in three steps. The paths of individual chromatids are especially well-defined by 3D visualization of axis component TopIIα. The 3D time-lapse imaging of axis signals during anaphase defines three sequential processes (Fig. 1*C*). This progression is illustrated for pig kidney cells expressing EGFP-tagged TopIIα (LLC-PK EGFP-TopIIα) in Fig. 2 *A–C*.

Global parallel separation. One or two minutes before sister chromatid centromeres begin to visibly move toward opposite poles, sister chromatid axes separate in parallel all along their lengths, in both arm(s) and centromere/kinetochore (hereafter referred to simply as "centromere") regions, globally throughout the chromosome complement (Fig. 2 *A* and *B*, t = 2 to 3 min; blue arrow).

Peeling apart. As centromere regions move toward opposite poles, this separation propagates outward along the arms, toward the telomere(s) (Fig. 2 *A* and *B*, t = 4 to 5 min; orange arrow). Concomitantly, regions distal to those undergoing peeling apart still remain parallel but continue to undergo modest further global separation (Fig. 2 *A* and *B*, t = 4 min).

Final resolution. After peeling apart is completed, sister chromatids move to widely separated positions near the poles. However, sister telomeres often remain visibly linked for some minutes (Fig. 2 *A* and *B*, t = 7 min) until finally separated.

The differential kinetics of global separation and peeling apart can be defined quantitatively (e.g., Fig. 2*C*). Global separation is defined by plotting interarm distances exclusively in regions that have not started to peel apart (Fig. 2*B*, dashed green and purple lines). Thus distances are defined along the entire length of a single chromosome before onset of peeling apart (e.g., t = 0 to t = 3 min); but after peeling apart has begun, distances are measured exclusively in distal regions that are still parallel (e.g., t = 4 min). Onset and progression of peeling apart are defined by measurement of intercentromere distances (yellow lines in Fig. 2*B*). The two plotted parameters are referred to as "parallel interarm distance" and "intercentromere distance," respectively (Fig. 2*C*).

Global separation and peeling apart can be seen with greater temporal resolution by two-dimensional (2D) single-plane images collected over shorter time intervals (e.g., every 2 s; selected images in Fig. 2*D*; all images in *SI Appendix*, Fig. S1 and Movie S1 and Fig. 2*E*). Global parallel arm separation (blue arrow) initiates about 1 min before onset of visible poleward movement of centromeres and peeling apart of arms from the centromere to the distal region(s) (orange arrow).

Global separation and peeling apart are also visible as distinct processes by imaging of chromatin (e.g., in DM87 Muntjac cells, which have very large chromosomes) (*SI Appendix*, Fig. S2) and in other cell types as described below.

Bridges are also removed in three stages. Imaging of chromosomes under conditions optimized for visualization of interaxis bridges reveals that bridges are altered, and then removed, in concert with the three stages of axis separation (Figs. 1*C* and 3 and *SI Appendix*, Fig. S4).

1) During global separation, bridges remain present but become slightly longer, in accord with increased separation of sister axes. There is no detectable change in the frequency; characteristically even spacing or overall morphologies of bridges as visualized by TopIIα or condensin I (Fig. 3 *A–D* and *H*).
2) During peeling apart, separation "forks" undergo a two-step progression. Bridges become dramatically elongated in a gradient from more to less centromere-proximal regions, with sisters now seen linked by connecting "strings" of TopIIα and condensin I (Fig. 3 *B*, *D–F*, and *H*). These strings are sometimes extremely prominent (Fig. 3*F*). The most highly elongated bridges then disappear. This sequence, occurring step by step along the chromosome arms, underlies progressive peeling apart.
3) Bridges tend to remain at telomeres for a prolonged period (Fig. 3 *A*, *B*, *D*, and *F*), pointing to special challenges to bridge disassembly in these regions. These telomere bridge linkages sometimes develop into the nearly invisible long-distance telomere connections that persist after bulk chromosome separation (Fig. 3 *D* and *E*, *G*, and *H*). We infer that long-distance telomere linkages are intrinsic features of normal anaphase separation and thus are distinct from so-called "ultrafine anaphase bridges," which appear to be pathological features (8, 9).

Universality. The three stages of sister separation are seen for axes and/or bridges and/or chromatin in three different species: 1) LLC-PK pig cells (which are telocentric, with the centromere at one end of each chromosome) (Figs. 2 *A–E* and 3 *A–F* and *SI Appendix*, Figs. S1, S4, S5, and S6); 2) two human cell lines (HeLa and HCT116) (metacentric) (Fig. 4 *C* and *E* and *SI*

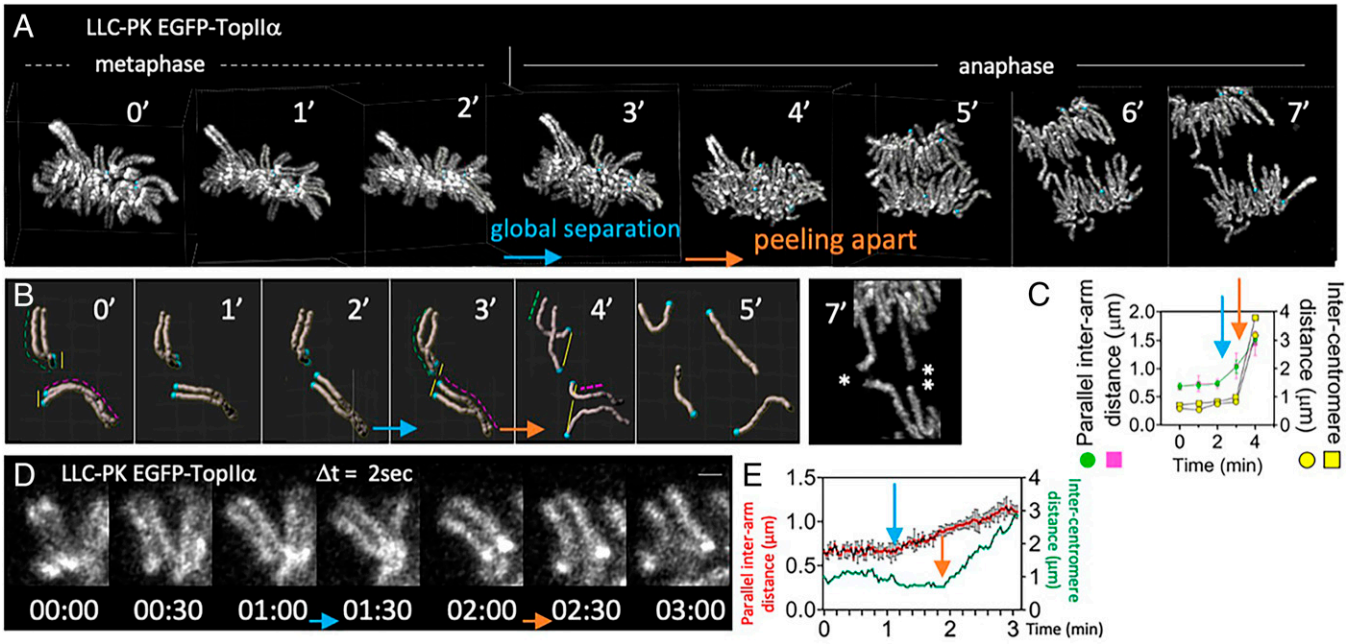

Fig. 2. Three morphological stages of anaphase sister separation defined by time-lapse imaging of chromosome axes illuminated with EGFP-TopIIα in LLC-PK cells. (*A–C*) Three-dimensional images illustrate global parallel separation, peeling apart, and final resolution of telomere linkages. (*A* and *B*) Images processed by Imaris software. (*B*) Two individual chromosomes were traced after extraction from the entire complement (*A*) and shown individually in random relative dispositions with centromeres marked by cyan dots. The *Right*-most image shows the chromosomes at t = 7 min: The two sisters are in the final stages of peeling apart (single asterisk) or have completed peeling apart but still appear connected at their ends (double asterisk). Importantly, at t = 7 min, the nucleus is at anaphase B, as indicated by the increased distance between the two poles as compared to t = 6 min (*A*). (*C*) Quantitative description of the first two stages of sister separation. Global separation is defined by the distance between sister axes in regions where those axes remain parallel (dashed green and purple lines in *B*). Onset and progression of peeling apart is defined by changes in intercentromere distance (yellow lines). Each curve corresponds to 3D distances obtained from one of the two chromosomes in *B*. Data for interarm distances are the average and SD for all distances along still-parallel regions: Entire chromosome at earlier times or remaining parallel regions during peeling apart (dashed lines in *B*). Each intercentromere distance comprises a single value for each given chromosome (thus without error bars). (*D* and *E*) Finer kinetics of separation revealed by 2D images and distance quantifications. Note tendency for sister centromere regions to approach one another before onset of peeling apart; basis unknown. See also Movie S1. Each parallel interarm distance data point is an average of at least 10 different distances; error bars denote SD. (Scale bars: 1 μm, solid line; 5 μm, dashed line.).

Appendix, Figs. S7 and S8); and 3) DM87 Muntjac cells (metacentric) (Fig. 3*H* and *SI Appendix*, Figs. S2, S4*G*, S16*A*, and S17). Global parallel separation is also dramatically apparent in Bajer's classical movies of giant Haemanthus (African Blood Lily) chromosomes (10, 11) (http://www.cellimagelibrary.org/images/11952) (*SI Appendix*, Fig. S3). Configurations corresponding to global separation and peeling apart were described for fixed, spread chromosomes of diverse mammalian cell types (12). And residual intertelomere linkages are a common feature of late anaphase (e.g., refs. 8, 9).

Part II. Cohesin Cleavage Licenses Global Separation and Peeling Apart.

All steps of sister separation are downstream of the spindle assembly checkpoint and the anaphase promoting complex–directed proteasome. The anaphase promoting complex (APC/C) ubiquitinates multiple protein targets, which thereby become substrates for degradation by the 26S proteasome (e.g., ref. 13). Activation of the APC/C, and thus downstream events, are inhibited by the spindle assembly checkpoint (SAC) until all chromosomes have achieved bipolar alignment on the spindle (e.g., refs. 14, 15).

The entire three-stage program of sister separation described above is downstream of the SAC and proteasome activity. SAC inactivation at metaphase, by addition of AZ3146 or reversine, results in coordinate acceleration of global parallel sister separation and peeling apart (*SI Appendix*, Fig. S5 *A–E*), because APC/C activation no longer has to wait for full chromosome alignment. Proteasome inactivation at metaphase, by addition of MG132, results in a block to global separation and peeling apart (Fig. 4 *A* and *B* and *SI Appendix*, Figs. S5 *D* and *E* and S6), even when the SAC is also inactivated (*SI Appendix*, Fig. S5 *D* and *E*).

Cleavage of cohesin licenses the sister separation program. After prophase, residual cohesin remains prominently at centromeres (16, 17) and also along interaxis bridges (6) (Fig. 1*A*). Sister separation requires cleavage of all of this residual cohesin by a specific protease, separase (18), which in turn is activated by the APC/C (e.g., ref. 19). Specifically, cleavage of cohesin is required for initiation of separation via global separation and for onset of peeling apart.

Expression of a transdominant mutant cohesin refractory to separase cleavage blocks global parallel separation. Cells carrying a gene for noncleavable cohesin under control of a doxycycline (Dox)-inducible promoter, plus EGFP-TopIIα, were treated (or not) with Dox in G1 and then imaged beginning at metaphase, 18 h later (*Materials and Methods*). In the absence of Dox, intersister axes undergo global separation after just a few minutes, as in other unperturbed situations above (Fig. 4 *C* and *D*, *Top* and *SI Appendix*, Fig. S7, *Top*). In contrast, in cells treated with Dox, chromosomes reach metaphase but remain in that conformation essentially indefinitely (>150 min; Fig. 4 *C* and *D*, *Bottom* and *SI Appendix*, Fig. S7, *Bottom*). Intersister arm distance remains constant at the distance seen in uninduced chromosomes prior to global separation (~0.75 μm) and TopIIα bridges retain their normal metaphase morphology, without initiating either global separation or peeling apart.

Conversely, if cohesin is artificially removed during prometaphase, thus well before APC/C activation and the normal time

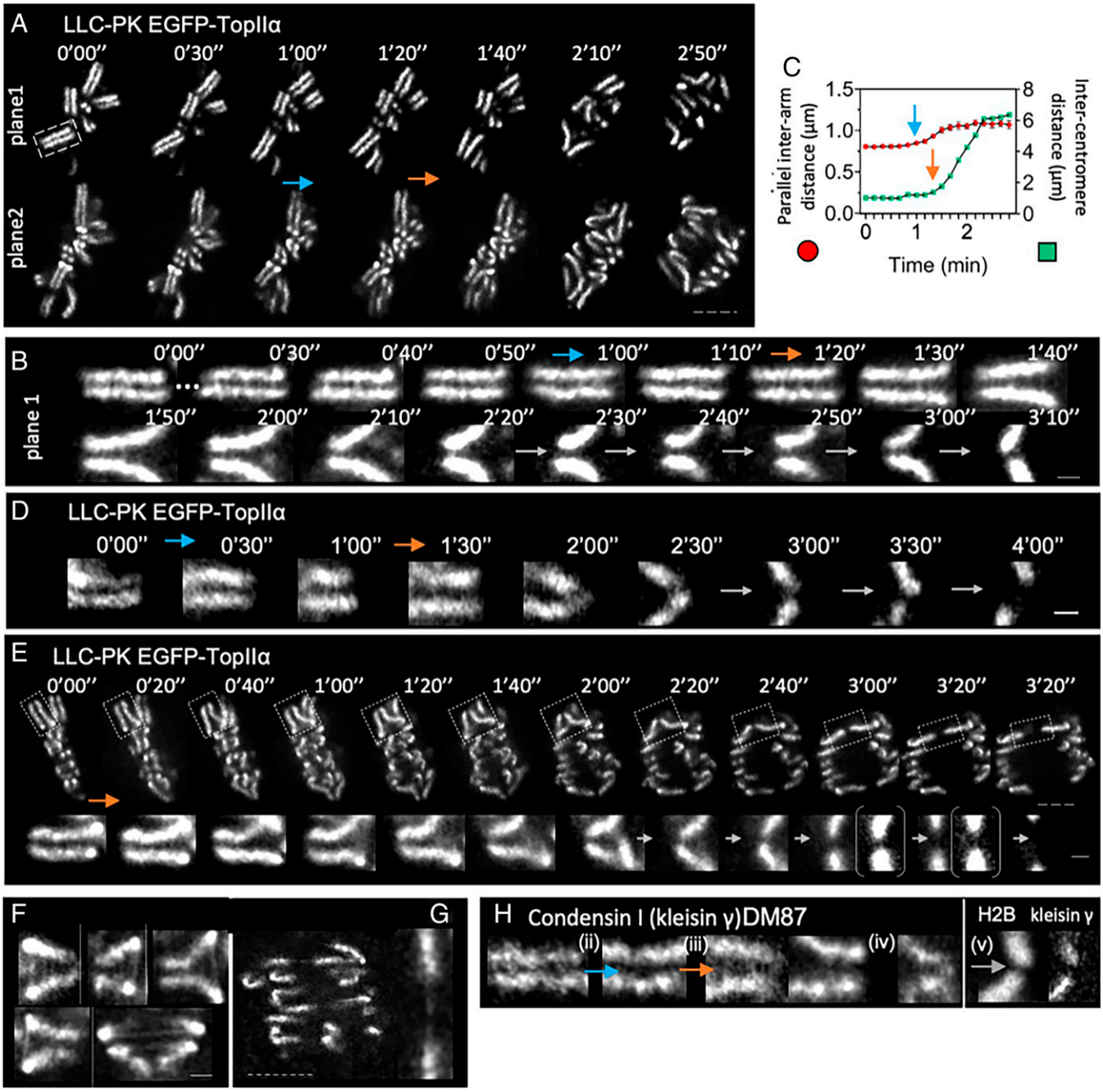

Fig. 3. Three morphological steps of bridge removal during anaphase sister separation defined by live cell imaging. Chromosomes illuminated with EGFP-TopIIα (*A*–*G*) or EGFP–kleisin-γ or H2B-GFP (*H*) in time-lapse series (*A*–*E*) or selected snapshots (*F*–*H*). Images illustrate whole nucleus (*A* and *E*, *Upper*, and *G*) and detailed (*B*, *D*, *E*, *Bottom*, *F*, and *H*) bridge morphogenesis during the three stages of sister separation (Fig. 1*C*). (*C*) Each interarm distance data point is an average of at least 10 different distances along the measured chromosome. Each intercentromere distance is a single data point. Error bars denote SD. (Scale bars: 1 μm, solid line; 5 μm, dashed line.).

of cohesin cleavage, sister arms immediately initiate global separation, without chromosomes ever achieving a metaphase configuration. This outcome was observed in a cell line expressing an auxin-inducible cohesin degron construct (*Materials and Methods*). In the absence of auxin, as usual, global parallel separation occurs ∼20 min after the end of prometaphase, with a metaphase chromosome configuration in place, and onset of peeling apart occurs ∼2 min thereafter (Fig. 4 *E* and *F*, *Top* and *SI Appendix*, Fig. S8, *Top*). By contrast, if auxin is added at prometaphase, the distance between sister arms begins to increase immediately and continues to increase progressively for ∼15 min, up to (and then beyond) the normal global separation distance (Fig. 4 *E* and *F*, *Bottom* and *SI Appendix*, Fig. S8, *Bottom*). In this condition, peeling apart is blocked due to activation of the SAC. Thus as soon as cohesin is removed, even before APC/C activation, global separation initiates immediately.

Cells treated with a proteasome inhibitor are known to finally begin to initiate peeling apart, dependent on microtubule forces, due to leakage through the block (the phenomenon of "cohesin fatigue") (20). We further find that, upon treatment with proteasome inhibitor MG132, global parallel separation of sister chromatid arms also finally begins to occur, e.g., 95 min

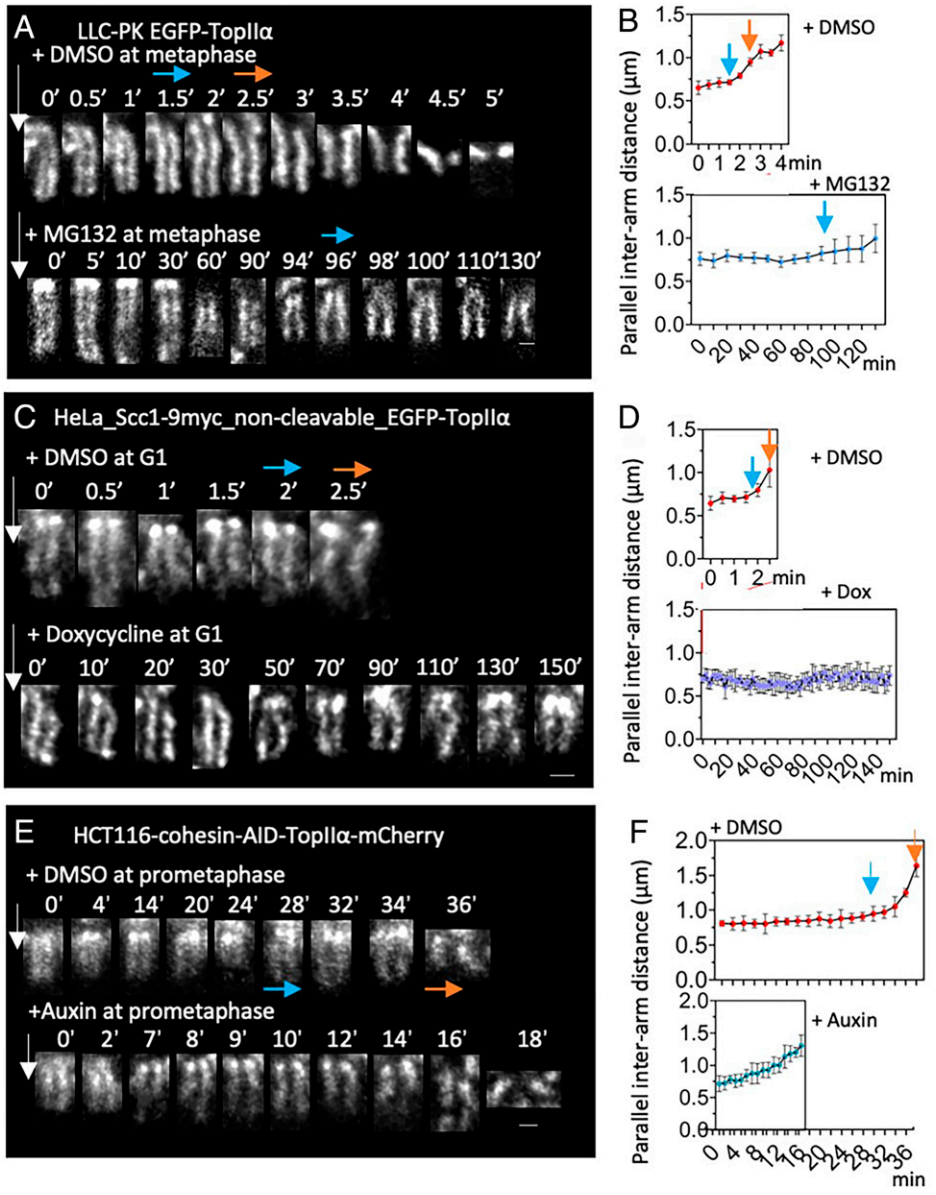

Fig. 4. Global separation is licensed by cohesin cleavage. Global parallel separation (blue arrows) and peeling apart (orange arrows) are both dependent upon the proteasome, as shown by addition of inhibitor MG132 at metaphase (*A* and *B*) (*SI Appendix*, Fig. S6). Both are also dependent upon proteasome-mediated cohesin removal (*C* and *D*). Oppositely, proteasome-independent removal of cohesin by auxin-induced degradation allows global separation (*E* and *F*), with peeling apart blocked due to activation of the SAC. Vertical white arrows indicate time of drug addition (defined as t = 0). Each interarm distance data point for each chromosome is an average of at least 10 different distances. Error bars denote SD. (Scale bars: 1 μm.).

after initiation of addition of inhibitor at metaphase (Fig. 4 *A* and *B* and *SI Appendix*, Fig. S6). Separation of sister centromeres and peeling apart eventually also occur, but lag behind. These effects can be explained by cohesin fatigue.

These findings point to cleavage of cohesin as the critical molecular trigger for onset of global separation as well as for onset of peeling apart. This sequential progression, and the prolongation of the time between the two events during cohesin fatigue, could both reflect the greater abundance of cohesin on centromeres versus bridges (*Discussion*).

Part III. Peeling Apart Is Promoted by Spindle Forces and Topoisomerase IIα. Microtubules (MTs) interact directly with kinetochores to promote movement of sister centromere/kinetochore regions to opposite poles (e.g., ref. 21). Microtubules also promote separation of sister chromatid arms by serving as guides for chromokinesins (reviewed in ref. 22). Sister chromatid separation also requires decatenation of chromatin loops, mediated by TopIIα (9). Decatenation is known to play essential roles at several stages of mitotic chromosome morphogenesis: For progression from G2 to prophase (23); for progression from midprophase to late prophase (when sister chromatids individualize and interaxis bridges emerge (17); and throughout prometaphase/metaphase, for normal chromosome compaction (24). Whether decatenation is required during anaphase per se has not been carefully examined. In addition, TopIIα is a prominent component of interaxis bridges (6) and, as such, must be removed during the process of bridge disassembly.

We have examined the roles of these players for anaphase sister separation by timed addition of an appropriate chemical inhibitor(s) and monitoring the consequences of their continued presence thereafter in real time. MTs are rapidly disassembled by addition of nocodazole (*SI Appendix*, Fig. S9). TopIIα activities can be inhibited by ICRF193. This drug traps the enzyme on the DNA in the "closed clamp" stage, thus block release/turnover of TopIIα binding to chromosomes, with concomitant inhibition of decatenation (25, 26). Accordingly, ICRF193 treatment increases the amount of TopIIα bound to postprophase chromosomes (*SI Appendix*, Fig. S11*A*). Effects of ICRF193 are visible in a minute or less after addition of the drug to the culture medium (17) and its effects are not attributable to rare induction of DNA damage (27).

Spindle forces are not required for global parallel sister separation but promote peeling apart. When MTs are disassembled by nocodazole treatment, global parallel separation is dramatically delayed and peeling apart is blocked (Fig. 5, compare lines 1 and 2). Since MT disassembly activates the SAC, these effects could potentially be indirect. However, inhibition of the SAC alone has no effect on sister separation except that all aspects are somewhat accelerated in time (Fig. 5, compare lines 1 and 3); and when cells are treated simultaneously with nocodazole plus an SAC inhibitor, global separation occurs normally but there is still no sign of peeling apart (Fig. 5, line 4 and *SI Appendix*, Fig. S10).

We infer that spindle forces are not required for global separation but are directly responsible for peeling apart. It is not rigorously excluded that global separation might be mediated by residual cytologically undetectable microtubules (e.g., via chromokinesins). However, the absence of any detectable effect of nocodazole on this phenotype makes this possibility seem unlikely. A role for microtubules in peeling apart is expected a priori, but these findings exclude alternative possibilities, e.g., a spreading change in internal chromosome structure independent of spindle forces (28).

ICRF193 treatment does not inhibit global parallel sister separation but blocks both onset and progression of peeling apart. In normally progressing cells, global parallel arm separation occurs ~20 min after appearance of the classic prometaphase "rosette" chromosome configuration (Fig. 6 *A* and *D* and *SI Appendix*, Fig. S11*B*, blue arrows). If ICRF193 is added at prometaphase, global separation still occurs, albeit with a very lengthy delay (Fig. 6 *B* and *D* and *SI Appendix*, Fig. S11*C*, blue arrows). This delay is due to activation of the SAC, a known but mysterious consequence specifically induced by treatment with ICRF193 (e.g., ref. 26), with eventual leakage through this block via cohesin fatigue (above). Correspondingly, when the SAC and TopIIα are both inhibited by simultaneous addition of the two corresponding inhibitors at prometaphase (Fig. 6*E* and *SI Appendix*, Fig. S11*C*), global separation now occurs in a timely fashion. However, onset of peeling apart is still completely blocked. Thus, ICRF193 treatment does not block global separation but does block onset of sister centromere separation.

Interestingly, onset of sister centromere separation becomes resistant to the effects of ICRF193 during mid/late metaphase. Addition of the drug to cells with a metaphase chromosome configuration produces two different outcomes: Type I, failure of peeling apart, just as seen for drug addition at prometaphase; and type II, onset of peeling apart, which, however, progresses only a short distance along the chromosomes. These same two phenotypes are observed both with and without inhibition of the SAC (Fig. 7). These two phenotypes represent the outcomes from addition of ICRF193 at early or mid/late metaphase, respectively, as indicated by the relative extents of

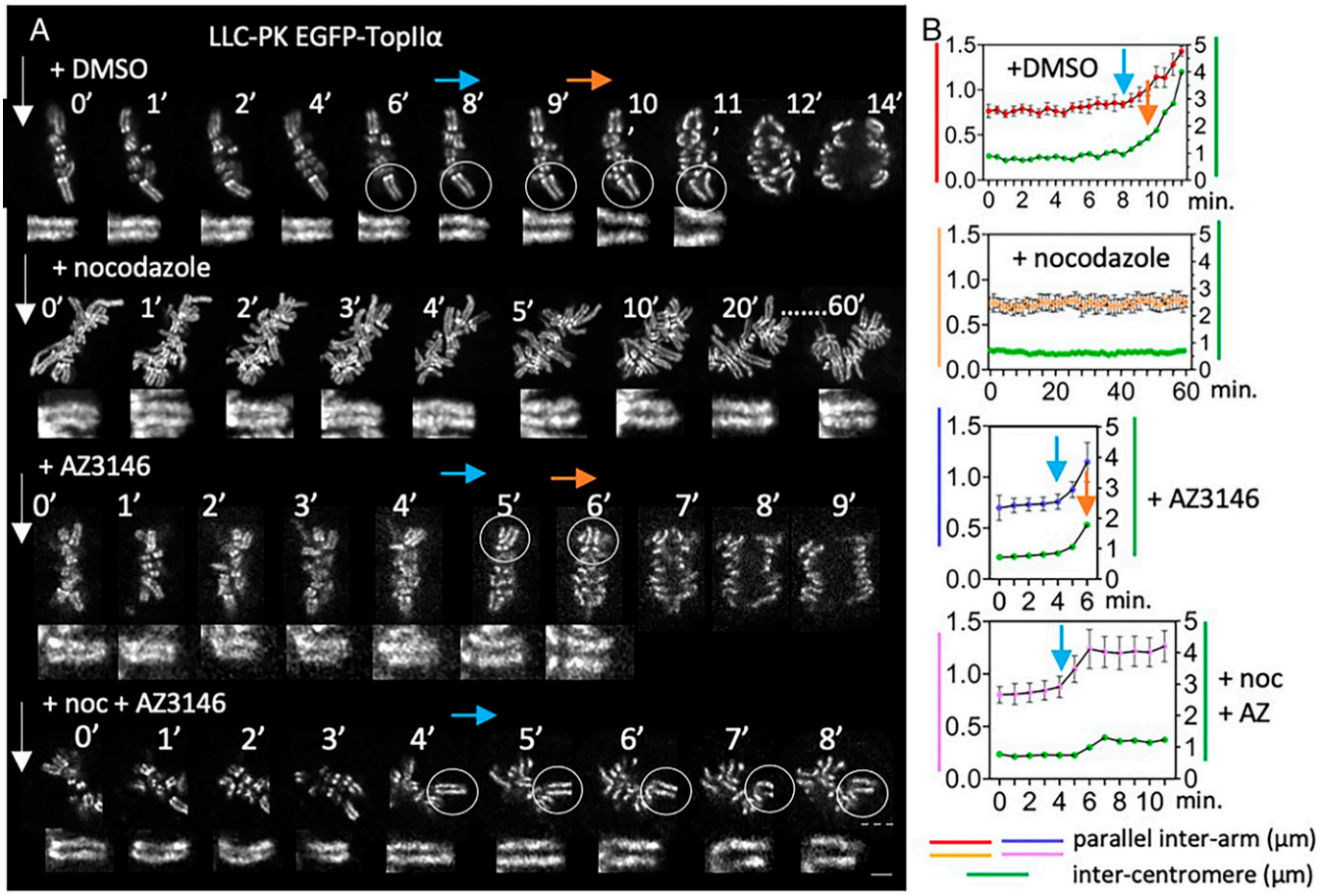

Fig. 5. Global separation is independent of spindle forces. Addition of nocodazole at metaphase blocks global separation (blue arrows) and peeling apart (yellow arrows) (*A* and *B*, *Second* row). Concomitant inhibition of the SAC (by AZ3146) alleviates the block to global separation (by allowing cohesin cleavage) but not microtubule-dependent peeling apart (*A* and *B*, *Bottom* row). Inhibition of the SAC alone (*A* and *B*, *Third* row from *Top*) (*SI Appendix*, Fig. S12) results in accelerated onset of both global separation and peeling apart. Vertical white arrows indicate time of drug addition (defined as t = 0). Each interarm data point is an average of at least 10 different interaxis distances; each intercentromere data point is one distance. Error bars denote SD. (Scale bars: 1 μm, solid line; 5 μm, dashed line.).

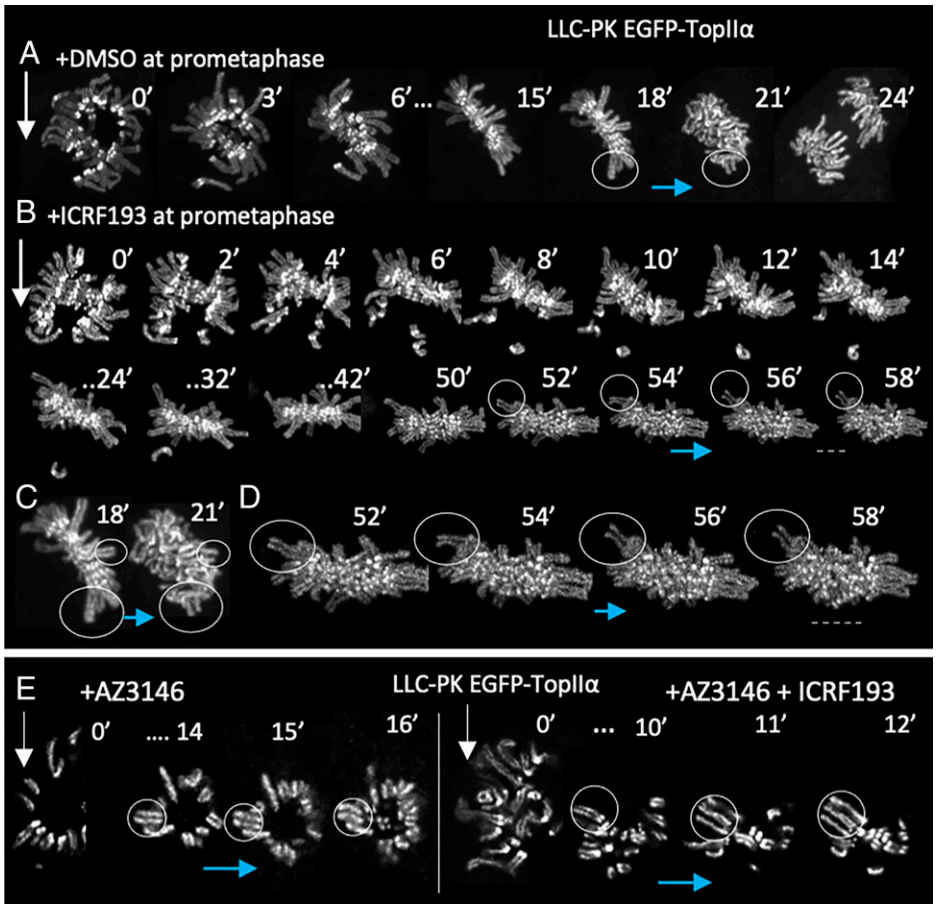

Fig. 6. Global separation is independent of TopIIα-mediated decatenation. (*A–D*) Global separation of sister chromatids (blue arrows) occurs despite the presence of ICRF193 added at prometaphase (thus well before onset of anaphase). Separation occurs with a long delay due to activation of the SAC (*A–D*) and in a timely fashion if the SAC is inactivated by simultaneous addition of AZ3146 (*E*). Plots of parallel interarm distances in *SI Appendix*, Fig. S11 *B* and *C*. Peeling apart does not initiate because it requires decatenation in centromere regions during mid/late metaphase (Fig. 7). White arrows indicate time of drug addition, defined as t = 0. (Scale bars: 5 μm.)

SAC-mediated delay and relative timing from drug addition to onset of global separation even in the absence of SAC activity (*SI Appendix*, Fig. S11*D*). Thus, centromere separation becomes resistant to the effects of ICRF193 at some point between early and late metaphase.

The type II phenotype also implies that ICRF193 can still block progression of peeling apart, even if it has already initiated. To further explore this possibility, we added ICRF193 to cells while peeling apart is in progress. We find that this process is virually stopped "in its tracks." Chromosomes arrest (or are dramatically delayed) with the same conformation normally observed at separation forks (Fig. 8 *A* and *B*).

This is a striking finding, for two reasons. First, it allows peeling apart to be divided into two successive processes (Fig. 8 *C–E*). Spindle forces that move sister centromeres to opposite poles promote elongation of bridges; and since chromatid axes are stiff, this effect propagates for some distance along the chromosome to decreasing extent with increasing distance. Then, elongated bridges are removed, dependent upon normal functioning of TopIIα. Put another way, normal functioning of TopIIα is required for the rate-limiting step(s) in poleward separation of sister chromatids at anaphase. The necessary steps likely involve both decatenation and TopIIα turnover (*Discussion*).

Second, this finding suggests that poleward separation of sister kinetochores is working against resistance from intersister bridges while waiting for bridge disassembly and decatenation to occur, with interesting implications (*Discussion*).

Long-distance telomere linkages are removed during anaphase B. In telomere regions, the bridge disassembly process is delayed and sometimes gives rise to long-distance barely/invisible linkages (above). Telomere effects can thus be explained if bridges are disassembled but intersister loops remain catenated. The corresponding intersister linkages would undergo dramatic elongation (e.g., by removal of histones or release from their axes) until eventually removed by TopIIα. Notably, these linkages remain present along only a subset of chromosomes, quite probably the longer ones. Furthermore, they are removed during anaphase B, during which period the spindle poles are moving apart from one another (Fig. 2 *A*, 7′, see legend; *SI Appendix*, Fig. S12) and chromosomes are undergoing dramatic compaction (29) (below). These effects could be important for promoting decatenation (*Discussion*).

Part IV. Global Separation Is Driven by Intersister Chromatin Pushing Forces. Global parallel separation of sister chromatids is independent of spindle forces and intersister decatenation. It does not involve bridge disassembly, but is nonetheless accompanied by bridge elongation (above). How is this transition accomplished? The answer to this question is suggested by investigation of the relationships among the chromatin and axis compartments along and between sister chromatids.

Chromatin and axes were imaged over time simultaneously using H2B-mCherry and EGFP-TopIIα, respectively (Fig. 9*A*, *Left*, *Middle* and *SI Appendix*, Fig. S13). For each chromatid along an individual analyzed chromosome, the paths of the intensity-weighted centroids for the chromatin and axis compartments were then determined, as described (6) (*Materials and Methods* and Fig. 9 *A*, *Right*). Notably, axis centroid paths exhibit pronounced half-helical handedness alternations ("perversions") as mirrored less dramatically in chromatin centroid paths (alternating red/blue and white/green centroid segments, respectively) (6, 7).

For each position along a set of chromosome centroids, a plane can be defined, which is perpendicular to the geometric

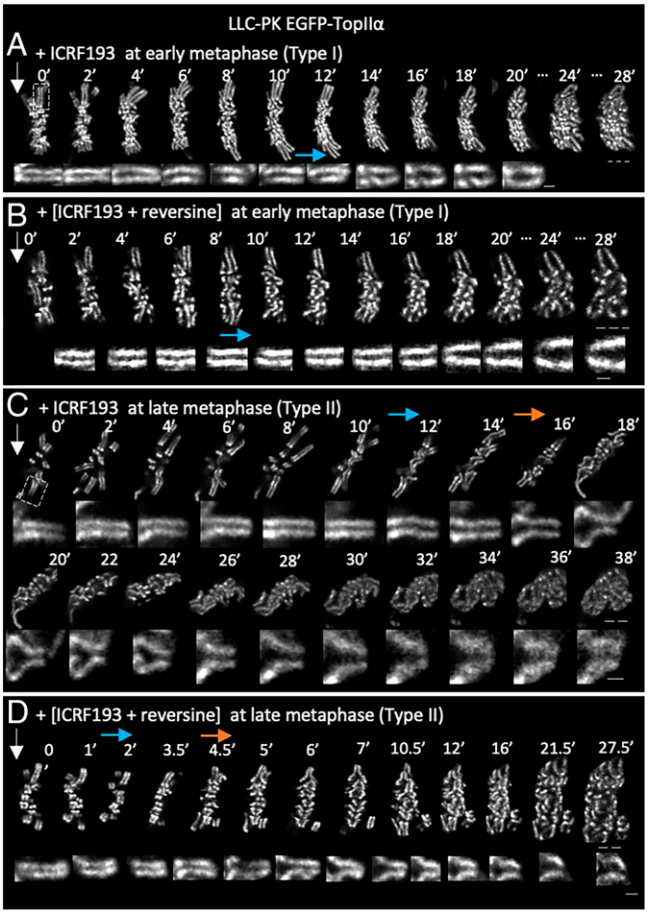

Fig. 7. Initiation of peeling apart requires TopIIα-mediated decatenation. Addition of ICRF193 to cells in early or late metaphase results in two different phenotypes: Type I (*A* and *B*) or type II (*C* and *D*). The type I phenotype is the same as when ICRF193 is added at prometaphase (Fig. 6); global separation occurs but peeling apart is not initiated. In the type II phenotype, in contrast, peeling apart initiates but progresses for only a limited distance before arresting with the same fork morphology seen throughout normal anaphase. Additional evidence suggests that type I and type II cells are at early metaphase and late metaphase, respectively, at the time of inhibitor addition and that the difference reflects the occurrence of decatenation within centromere regions at mid/late metaphase (*SI Appendix*, Fig. S11*D*). The same two phenotypes occur with a delay if ICRF193 is added alone (*A* and *C*) and in a timely fashion if SAC inhibitor reversine is added at the same time (*B* and *D*). Thus, inhibition of decatenation during metaphase activates the SAC. SAC activation is more or less severe in type I and type II cells (*SI Appendix*, Fig. S11*D*). White arrows indicate time of drug addition, defined as t = 0. (Scale bars: 1 μm, solid line; 5 μm, dashed line.).

axis defined by the vector linking the two TopIIα–TopIIα centroids at that position (Fig. 9*B*). The positions of the H2B and TopIIα centroids for each sister within this plane are experimentally defined, able to specify the vectors that link the two centroids within each chromatid (TH1 and TH2) and the interchromatid distances between the chromatin and axis centroids on the two sisters (D_{HH} and D_{TT}, respectively) (Fig. 9 *C* and *D*). Given this frame of reference, centroid relationships can be defined relative to the chromosome's bridge/axis/bridge plane despite a tendency for slight twisting of the chromosome along its length.

Sister chromatid loop/axis arrays rotate from opposing to parallel configurations during global separation (and further rotate during peeling apart). Onset of global parallel separation is manifested in a dramatic increase in the separation of sister axis (TopIIα) centroids (above) (increased D_{TT}; Fig. 9 *E*, *i*, vertical blue line). Increased separation of sister chromatin H2B centroids (increased D_{HH}) also occurs (Fig. 9 *E*, *i*). However, unexpectedly, the relationship between the two distances, D_{TT} and D_{HH}, and thus their ratio, changes over time (Fig. 9 *E*, *i* and *ii*). Prior to onset of global separation, D_{HH} is greater than D_{TT}, giving D_{HH}/D_{TT} greater than one. At onset of global separation, D_{TT} increases more rapidly than D_{HH} until D_{HH} and D_{TT} are very similar and D_{HH}/D_{TT} stabilizes around one. Finally, around the time of peeling apart, D_{TT} tends to be greater than D_{HH}, giving D_{HH}/D_{TT} less than one. These patterns are seen as average values within a selected internal segment (Fig. 9 *A*, *Right* and *E*), and along whole chromosome lengths, in several independent time series ($n = 5$) (*SI Appendix*, Figs. S14 and S15).

The basic loop/axis array along each chromatid remains present throughout this period, with no morphological changes visible to the eye (e.g., Fig. 9 *A* and *B* and above). Given this constraint, the observed effects could be explained by rotation of sister loop/axis arrays relative to one another (Fig. 9*F*). In this scenario, sister-chromatid chromatin arrays would initially tend to point away from each other (giving $D_{HH} > D_{TT}$). At the global separation transition, increased distance between sister-chromatid axes would be accompanied by a tendency for sister loop/axis arrays to be oriented in parallel (giving $D_{HH} = D_{TT}$). Finally, during peeling apart, there would be a tendency for complete inversion of the relationship, with sister chromatin arrays pointing inward and axes pointing outward (giving $D_{HH} < D_{TT}$).

This scenario can be assessed by analyzing the relative orientations of the two intrachromatid axis-chromatin vectors (TH1 and TH2) using an appropriate coordinate system (Fig. 9*G*). In brief, within each position-specific plane where the ordinate is the trajectory between the two TopIIα centroids (above), two perpendicular abscissas run through these two centroids, and the conventions for the signs of angles and vectors for the two sister chromatids are defined in a mirror symmetric fashion. The rotational relationship between the TopIIα-chromatid centroid vectors of sister chromatids is reported by defining the vectors describing their projections onto the ordinate (a1 and b1) and determining their sum (a1 + b1). If sister vectors are pointing away from each other, (a1 + b1) will be negative; if they are pointing in parallel, (a1 + b1) will be zero; and if they are pointing toward one another, (a1 + b1) will be positive. We observe that, in accord with the rotation scenario above, (a1 + b1) is negative prior to global separation, increases to zero at global separation, and is positive around the time of peeling apart (Fig. 9 *E*, *iii* and *SI Appendix*, Figs. S14 and S15). Control comparisons demonstrate that variations in the lengths of the TH1 and TH2 vectors (below) make only small contributions to these patterns.

Further analysis reveals that the distance between the TopIIα and H2B centroids within each chromatid (TH1, TH2) (Fig. 9*G*) increases about 1 min prior to onset of global separation, reaches a maximum at exactly the time of global separation as defined by the onset of an increase in D_{TT} and a decrease the D_{HH}/D_{TT} ratio, and then decreases back to its original preincrease (metaphase) value (Fig. 9 *E*, *iv*) vs. blue line. Sister chromatids tend to undergo these changes coordinately (Fig. 9 *E*, *iv*). This pattern suggests that chromatin loops transiently become elongated in a direction away from their axis before returning to their original nonelongated state. A second increase and decrease in TH1 and TH2 occurs while peeling apart is in progress (Fig. 9 *E*, *iv* vs. orange line). These dynamic modulations of TH1 and TH2, like the interchromatid effects described above, are seen in multiple independent datasets (*SI Appendix*, Figs. S14 and S15).

All of the above effects, while apparent in per-segment and per-chromosome averages, do vary in detail along the lengths of the chromosomes. Along an individual chromatid, rotation occurs coordinately over distances of ~0.5 μm or more, with no obvious

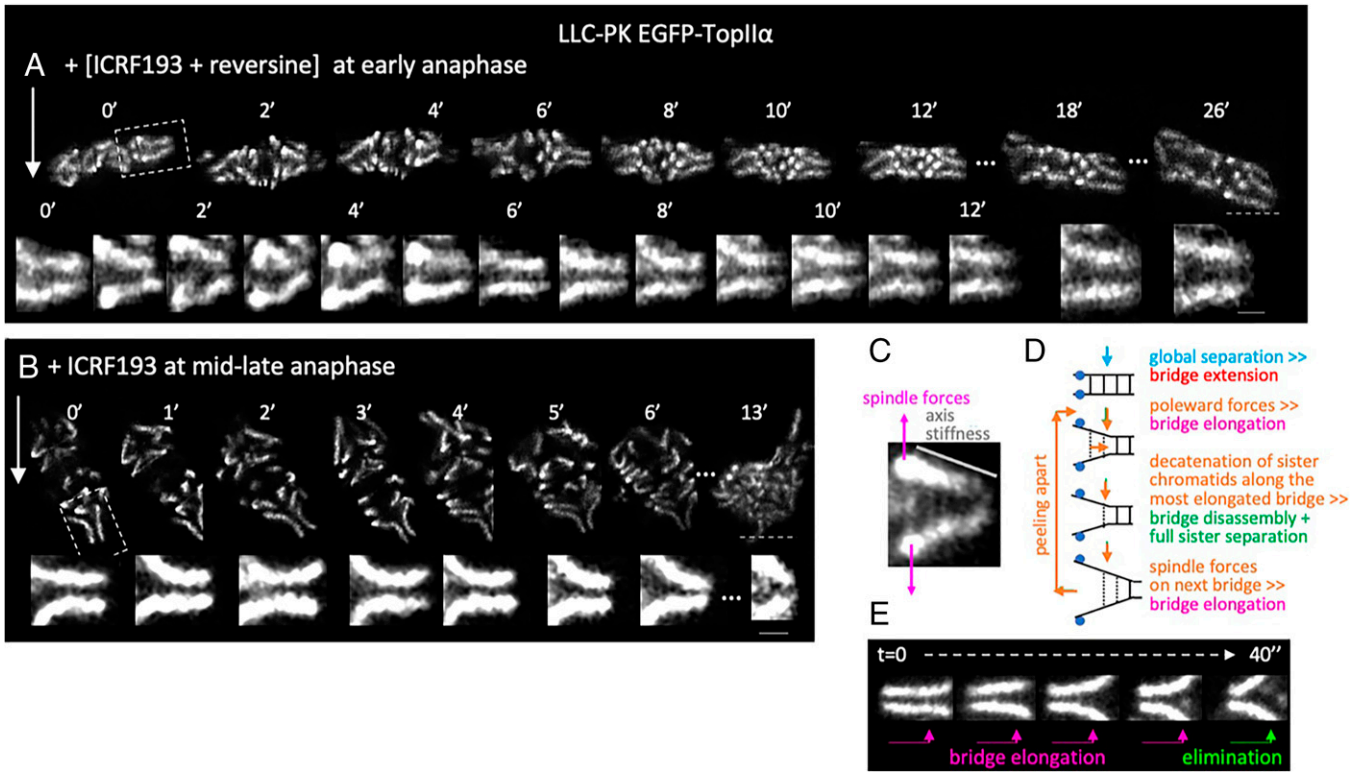

Fig. 8. TopIIα-mediated decatenation is the rate-limiting step in peeling apart. (*A* and *B*) When ICRF193 is added when peeling apart is in progress, that process is stopped in its tracks (except that eventually, after many minutes, forks open up to give hyperelongated bridges). White arrows indicate time of drug addition, defined as t = 0. (*C*–*E*) Model for peeling apart. (*C*) Spindle forces promote separation of axes proximal to the centromeres, causing bridge elongation. Since the axes are stiff, this effect is propagated for some distance along the chromosome. (*D*) Full scenario: During peeling apart, spindle forces cause extensive bridge elongation, thereby making the component sister chromatid catenations subject to decatenation by TopIIα. (*E*) Morphologies corresponding to the steps of peeling apart outlined in *D*. (Scale bars: 1 μm, solid lines; 5 μm, dashed lines.).

tendency for coordinate changes on sister chromatids. Full analysis of these and other effects awaits a greater sample size.

Explanation. An unconstrained polymer in a given state tends intrinsically to occupy a characteristic "envelope volume." DNA/chromatin will therefore tend to expand as much as possible, toward that volume, to the extent permitted by constraining features. Furthermore, if adjacent chromatin loops, or arrays of loops, are spatially constrained, they will tend to push against one another ("chromatin pressure"); and if those constraints are removed, the loops will tend to push one another farther apart (30, 31). This effect is illustrated by previous findings regarding individualization of sister chromatids at late prophase. In this case, when bulk cohesin is removed, sister chromatin compartments push one another apart (17).

During prometaphase/early metaphase the chromatin arrays of sister chromatids become progressively "fatter," because chromatin loops become longer and fewer (6, 32). Bridge lengths increase, but to a barely discernible extent. As a result, fatter sister chromatin arrays push each other apart into a configuration in which chromatin centroids are more widely separated than axis centroids, thus explaining why $D_{HH} > D_{TT}$.

During global separation, sister loop/axis arrays rotate into a parallel configuration (Fig. 9 *E* and *F*). Concomitantly, bridges elongate (above). These coordinate effects are explained if bridges have become more extendable (e.g., due to loss of cohesin; *Discussion*), thereby allowing interchromatin pushing forces to produce the lower energy side-by-side relationship, with axes responding to become more widely separated. This scenario explains the fact that interaxis and interchromatin centroid distances become exactly the same ($D_{HH}/D_{TT} \sim 1$), which otherwise would involve ad hoc assumptions. The requisite change in the physical properties of bridges can be attributed to loss of bridge-associated cohesin, which triggers the global separation transition (*Discussion*). In summary, global separation of axes is driven by intersister chromatin pushing forces as licensed by cleavage of cohesin on bridges.

If pushing forces between sister-chromatid chromatin arrays are responsible for global separation, such an effect would be enhanced by any additional overall increase in chromatin volume. Increased volume would increase the amount of pushing force, and thus the energy available to promote rotation into a parallel configuration, thereby making the global separation transition more energetically favorable (Fig. 9*H*). It would also increase the tendency for this rotation to occur in a concerted fashion along the length of a chromosome. Two lines of evidence suggest that such an effect occurs. First, it could explain the accompanying transient increase in TH1 and TH2. Expansion in the longitudinal direction, along an axis, is precluded by the presence of closely packed adjacent chromatin loops, which will resist by "pushing back." Thus, an expansion tendency will be manifested in nonisometric extension away from the axis, giving an increase in TH1 and TH2 (Fig. 9*H*). Furthermore, this tendency will be alleviated if chromatin pushing drives rotation of sister chromatid loop/axis arrays into a more parallel, lower energy orientation (thus giving global separation) (Fig. 9*H*). Second, global chromosome volume increases during early/mid anaphase, in tight temporal correlation with global separation and continuing through peeling apart, before decreasing once peeling apart is completed, at the onset of anaphase B, as seen in both Muntjac and pig cells (*SI Appendix*, Figs. S16–S18). The molecular basis for this global expansion remains to be determined, but a change in nucleosome state is one possibility (33).

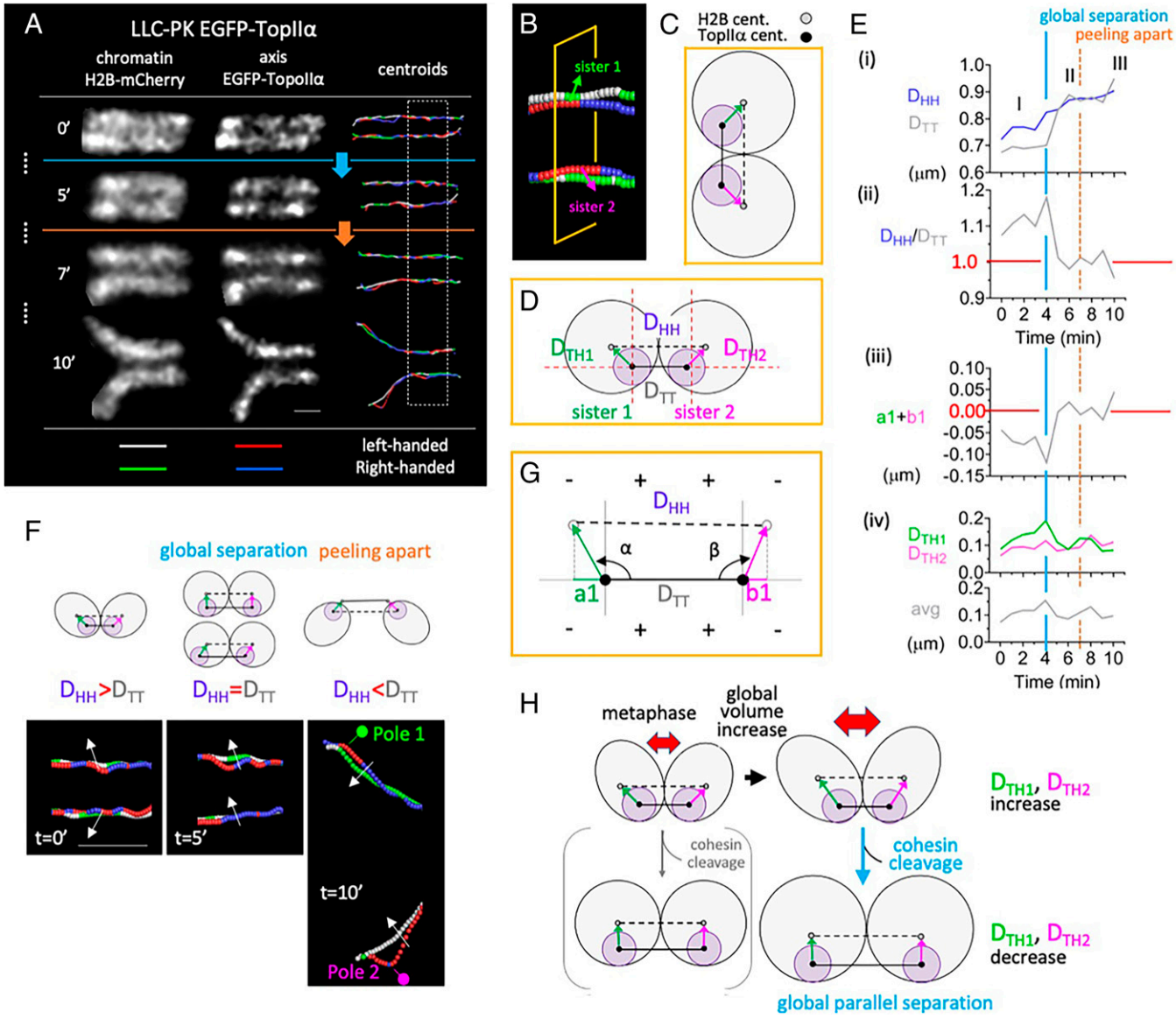

Fig. 9. Global separation is driven by intersister chromatin pushing forces. (*A*) Three-dimensional time-lapse images acquired simultaneously for chromatin (*Left*) and axis markers (*Middle*) of a chromosome in a living LLC-PK cell as it progresses from metaphase through midanaphase and corresponding intensity-weighted centroids (*Right*, obtained as in ref 6). Adjacent balls along a centroid path corresponds to adjacent positions along the horizontal (*y*) axis. Centroid relationships were analyzed both for the entire chromosome and for a selected internal region (white dashed rectangle). (Scale bars, 1 μm.) (*B–D*) At each centroid position, a plane perpendicular to the long axis of the chromosome was defined (gold box), and, within that plane, for each chromatid, the vector that links the TopIIα centroid to its partner H2B centroid (green and pink arrows) was defined. The lengths of the two chromatid loop/axis vectors (D_{TH1} and D_{TH2}) and the distances between the corresponding centroids of the two sisters (D_{TT} and D_{HH}) were then determined. (*E*) Values of the indicated parameters, averaged over all positions along the internal chromosome segment selected in *A*, were plotted as a function of imaging time. Analogous plots for the entire chromosome and for both selected segments and entire chromosomes in four other samples are shown in *SI Appendix*, Figs. S14 and S15. (*F*) The relationships between D_{TT} and D_{HH} as defined in *E*, *i* and *E*, *ii* can be explained if the rotational relationships between sister loop/axis arrays change relative to one another over time, in two transitions (I–II and II–III), which correspond, respectively, to the onset of global separation (*Middle*) and the onset of peeling apart (*Right*). (*G*) The scenario of *F* was evaluated by defining, at each position along a chromosome, the projections of each chromatid TopIIα-H2B vector onto the bridge/axis/bridge plane with corresponding signs defined with mirror symmetry for the two sisters (a1 and b1). In this coordinate system, the tendency for the two vectors to point away from one another, to be parallel, or to point toward one another (as in *F*) is given by their sum (a1 + b1), which will be negative, zero, or positive in the three cases. (*H*) Model for how loop/axis shapes and intersister relationships might evolve during global separation. *Top Left*: Prior to the onset of global separation, sister loop/axis arrays point away from one another because bridges hold axes close together, forcing chromatin to the outside so as to minimize chromatin pressure. *Top Right*: Prior to cohesin cleavage, a global volume increase will force elongation of chromatin loops away from the constraints of the bridge-linked axes. *Bottom Left and Right*: Cleavage of cohesin will weaken bridges such that chromatin pressure will be strong enough to push axes farther apart, with concomitant bridge elongation (black line), thus producing a more energetically favorable chromatin configuration that now dictates axis/bridge/axis relationships. This effect will be more efficient and dramatic if it is preceded by a global volume increase (*Right* versus *Left*).

Finally, inversion of sister loop/axis disposition during peeling apart, to D_{HH}/D_{TT} <1, can be explained by a different effect. If kinetochores are built on chromosome axes, as would be structurally sensible (34), the spindle forces that move sister kinetochores in opposite directions will automatically cause sister arrays to turn "inside out." This effect can be seen directly,

e.g., in Fig. 9*F*: axes initially tend to be internal (*Left*; vectors pointing outward away from one another), then become parallel (*Middle*; vectors pointing in the same direction) and, finally, may be located externally (*Right*; vectors pointing inward, toward one another, implying that sister axes are oriented outward toward the two poles).

Discussion

The present study reveals a high-resolution temporal, morphological, and functional view of how sister chromatids segregate to opposite poles at anaphase. The findings define a highly programmed process mediated by robust interaxis bridges, contradicting the widespread early impression that sister chromatid arm separation involves resolution of linkages at the peripheral chromatin/chromatin interface. The described program appears to be widely conserved among mammals and plants.

Three Morphological Stages of Sister Chromatid Separation. During anaphase, three morphological stages occur in succession (Fig. 1*C*): Global separation of sister chromatids along their lengths; peeling apart of sister chromatids, which initiates at the centromere and progresses to telomere(s); and finally, resolution of long-distance telomere linkages. All events are downstream of anaphase-specific regulation by the SAC, the APC/C, and the 26S proteasome. All three stages are accompanied by characteristic morphological changes in interaxis bridges. Bridges become modestly longer during global separation. During peeling apart, bridges become dramatically elongated at separation forks and then disappear, with concomitant wide separation of sister chromatid arms. Finally, at some telomeres, long-distance linkages emerge from bridges that have otherwise disassembled and are finally resolved.

Three Stage-Specific Intersister Separation Forces. The three stages of axis separation have different functional requirements, implying different underlying mechanisms. Nonetheless, it seems that each of the three phases is driven by its own, stage-specific, intersister separation force.

Global separation is driven by the internal forces of chromatin pushing between sister chromatids, independent of spindle forces, and insensitive to inhibition of TopIIα activities by ICRF193. The effects of pushing are apparently enabled by the enhanced ability of bridges to elongate in the absence of cohesin and enhanced by a global increase in chromatin volume, a parallel feature of the anaphase program (above). Ultimately, spatial chromatin reorganization should be driven by thermal forces as licensed by release of tethers (33).

Peeling apart is driven by poleward spindle forces, which cause bridges to dramatically elongate and then, finally, disappear. ICRF193 arrests this peeling apart process in its tracks, implying a critical rate-limiting role for either TopIIα removal and/or TopIIα-mediated decatenation. Given the known effects of ICRF193 addition (above), and the likelihood that catenations are embedded within the context of the bridges (Introduction) it seems likely that the primary basic force-mediated effect is bridge disassembly, dependent on removal of TopIIα. Sister decatenation could be directly coupled to this process and/or could occur as a separate, subsequent step. These considerations further imply that when peeling apart is in progress, poleward movement of kinetochores should be working against resistance from intersister bridges. This effect, in turn, should ensure that sister chromatids move synchronously and smoothly toward their respective poles. A previous study suggested that cohesin provides the primary barrier to microtubule force–mediated separation of sister chromatids (35). The current work suggests that, in contrast, during peeling apart, the operative barrier is bridge removal, which is downstream of cohesin release. The same could be true at centromeres.

Long-distance telomere linkages presumptively represent residual catenations between sister chromatid loops. Correspondingly, these linkages might represent cases in which bridges were disassembled but without normal accompanying (coupled) decatenation as occurs during peeling apart in arm regions. Aberrant disassembly could be reflected in stalling of peeling apart in telomere regions. Residual linkages could potentially occur primarily on longer chromosomes. We suggest that decatenation requires pulling of sister chromatid loops in opposite directions. The requisite tension could be provided either by increased pole-to-pole distance (anaphase B) and/or chromosome compaction, both of which are characteristic of this stage (above) (29).

Cohesin Loss Triggers and Enables Bridge Elongation to Allow Arm Separation. Global separation and peeling apart (and thus final resolution of telomere linkages) both require cohesin cleavage by separase. Since cohesin is present uniquely on bridges and centromere regions at this stage (Introduction), cleavage of cohesin would appear to be the critical trigger for separation in both regions. Lower versus higher abundance of cohesin on bridges versus centromere regions could thus explain why global separation precedes onset of peeling apart, initiated at centromeres, by about 1 min. Thus, cohesin release may be the critical determinant of the onset, relative timing, and the execution of both phases, thereby expanding the special transitional role of this molecule during anaphase.

Along chromatid arms, we propose that cleavage of the cohesin on bridges allows them to elongate in response to intersister chromatid separation forces during global separation and peeling apart, and that this effect ultimately renders the underlying intersister catenations susceptible to the action of TopIIα during peeling apart and, then, during finalization of separation. We cannot, of course, exclude that undetectable levels of cohesin also occur in the peripheral chromatin and thereby are also relevant to segregation; however, there is no experimental evidence to that effect, and the amount of cohesin on bridges is already very small (6, 18).

Interestingly, a constraining role for cohesin on bridges, as released during anaphase, would be analogous to that observed globally along the chromosomes at late prophase (17). At this stage, cohesin is released in bulk from the chromosome axes prior to separase cleavage, thereby allowing sister axes to separate, via intersister chromatin pushing forces, to give sister individualization (plus concomitant emergence of interaxis bridges).

The current findings also highlight the question of how the starting configuration of bridge-associated cohesin is set up at late prophase during emergence of bridges. Why, after cohesin is lost in bulk at early/mid prophase, is this molecule nonetheless retained specifically on bridges (and in centromere regions)? It is tempting to suggest that the critical factor is a tendency for cohesin to localize to sites of intersister catenation (which may also be nucleosome-free regions, as seen for anaphase cohesin binding in yeast) (36). Bridges comprise essentially the same components as chromosome axes, with two exceptions: Cohesin and intersister catenations (versus intrachromatid catenations along the main axes), and bridges could be built on those catenations (Introduction). Moreover, we find that centromere regions, which have high levels of cohesin, seem also to have intersister catenations that are removed during metaphase. These scenarios are also consistent with evience from budding yeast, where cohesin is thought to "lock in" intersister catenations (4).

Is TopIIα-Mediated Decatenation Directly Dependent on Intersister Separation Forces? A striking feature of this program is the prominent role of TopIIα. Removal of this molecule and/or its role in decatenating sisters is required for both progression of

peeling apart and (presumptively) for resolution of late-persisting links in telomere regions. Most importantly, during peeling apart, TopIIα mediates an integral mechanistic feature, which seems to be the rate-limiting step for sister arm separation. It is also required for onset of peeling apart, and thus for separation of sister centromere regions, during late metaphase, prior to global separation. We note, however, that we cannot rigorously exclude the possibility that these effects are accentuated by reduction or alteration in the TopIIα activities of the EGFP-TopIIα construct, which is used to detect detailed effects.

We find it interesting that during the two stages when decatenation is important, i.e., peeling apart and late resolution of telomere linkages, catenated sister loops are being actively pulled in opposite directions, by spindle forces during/after bridge disassembly, and potentially by events of anaphase B, respectively (above). Perhaps these effects are required only to provide directionality to the reversible catenation/decatenation reaction. However, an intriguing additional possibility is that pulling of sister loops in opposite directions has a more active role, e.g., by promoting the bent DNA geometry required for TopIIα function (37).

Bridges as Topological Gatekeepers of Mitotic Chromosomes. Bridges are important during prometaphase/metaphase to ensure that sister chromatids remain in a regular topological relationship, side by side, without helical coiling, during the turbulence of chromosome compaction (6). If poleward movement of sister kinetochores is working against resistance due to intersister bridges (above), bridges should be directly, mechanistically important for ensuring that sister kinetochores move smoothly toward their respective poles, in a directed fashion, with sister kinetochores remaining oppositely oriented, rather than being allowed to oscillate; and this effect would concomitantly ensure that poleward movement and separation occur synchronously and regularly on the two sister chromatids. Overall, these effects suggest that interaxis bridges could be the topological gatekeepers of mitotic chromosomes not only before and during compaction, but also during anaphase segregation, and thus throughout the entire mitotic chromosomal program.

Materials and Methods

For information on plasmids, cell lines, cell culture, synchronization, transfection, imaging, cell line generation by CRISPR, Western blot, and measurement, please refer to *SI Appendix, Materials and Methods*.

Data Availability. All data and materials are available as described in the article and *SI Appendix*.

ACKNOWLEDGMENTS. We thank Andrew Seeber (Harvard Center for Advanced Imaging) for access to his spinning-disk microscope and Houqing Yu for help with Western blots. This research was supported by grants to N.K. from the NIH (R35-GM-136322) and to Z.Z. from the National Natural Science Foundation of China (No. 31900024).

1. J. F. Giménez-Abián *et al.*, Regulation of sister chromatid cohesion between chromosome arms. *Curr. Biol.* **14**, 1187–1193 (2004).
2. M. Nakajima *et al.*, The complete removal of cohesin from chromosome arms depends on separase. *J. Cell Sci.* **120**, 4188–4196 (2007).
3. S. M. Germann *et al.*, TopBP1/Dpb11 binds DNA anaphase bridges to prevent genome instability. *J. Cell Biol.* **204**, 45–59 (2014).
4. A. M. Farcas, P. Uluocak, W. Helmhart, K. Nasmyth, Cohesin's concatenation of sister DNAs maintains their intertwining. *Mol. Cell* **44**, 97–107 (2011).
5. J. F. Giménez-Abián *et al.*, DNA catenations that link sister chromatids until the onset of anaphase are maintained by a checkpoint mechanism. *Eur. J. Cell Biol.* **81**, 9–16 (2002).
6. L. Chu *et al.*, The 3D topography of mitotic chromosomes. *Mol. Cell* **79**, 902–916.e6 (2020).
7. L. Chu *et al.*, One-dimensional spatial patterning along mitotic chromosomes: Perversions and bridges. *Proc. Natl. Acad. Sci. U.S.A.* **117**, 26749–26755 (2020).
8. A. Finardi, L. F. Massari, R. Visintin, Anaphase bridges: Not all natural fibers are healthy. *Genes (Basel)* **11**, 902–930 (2020).
9. R. Broderick, W. Niedzwiedz, Sister chromatid decatenation: Bridging the gaps in our knowledge. *Cell Cycle* **14**, 3040–3044 (2015).
10. A. Bajer, J. Molè-Bajer, Cine-micrographic studies on mitosis in endosperm. *Chromosoma* **7**, 558–607 (1955).
11. S. Inoué, R. Oldenbourg, Microtubule dynamics in mitotic spindle displayed by polarized light microscopy. *Mol. Biol. Cell* **9**, 1603–1607 (1998).
12. J. F. Giménez-Abián *et al.*, Regulated separation of sister centromeres depends on the spindle assembly checkpoint but not on the anaphase promoting complex/cyclosome. *Cell Cycle* **4**, 1561–1575 (2005).
13. S. Sivakumar, G. J. Gorbsky, Spatiotemporal regulation of the anaphase-promoting complex in mitosis. *Nat. Rev. Mol. Cell Biol.* **16**, 82–94 (2015).
14. J. Nilsson, M. Yekezare, J. Minshull, J. Pines, The APC/C maintains the spindle assembly checkpoint by targeting Cdc20 for destruction. *Nat. Cell Biol.* **10**, 1411–1420 (2008).
15. A. Musacchio, E. D. Salmon, The spindle-assembly checkpoint in space and time. *Nat. Rev. Mol. Cell Biol.* **8**, 379–393 (2007).
16. I. C. Waizenegger, S. Hauf, A. Meinke, J. M. Peters, Two distinct pathways remove mammalian cohesin from chromosome arms in prophase and from centromeres in anaphase. *Cell* **103**, 399–410 (2000).
17. Z. Liang *et al.*, Chromosomes progress to metaphase in multiple discrete steps via global compaction/expansion cycles. *Cell* **161**, 1124–1137 (2015).
18. S. Hauf, I. C. Waizenegger, J. M. Peters, Cohesin cleavage by separase required for anaphase and cytokinesis in human cells. *Science* **293**, 1320–1323 (2001).
19. I. Waizenegger, J. F. Giménez-Abián, D. Wernic, J. M. Peters, Regulation of human separase by securin binding and autocleavage. *Curr. Biol.* **12**, 1368–1378 (2002).
20. J. R. Daum *et al.*, Cohesion fatigue induces chromatid separation in cells delayed at metaphase. *Curr. Biol.* **21**, 1018–1024 (2011).
21. M. I. Anjur-Dietrich, C. P. Kelleher, D. J. Needleman, Mechanical mechanisms of chromosome segregation. *Cells* **10**, 465–489 (2021).
22. A. C. Almeida, H. Maiato, Chromokinesins. *Curr. Biol.* **28**, R1131–R1135 (2018).
23. C. S. Downes *et al.*, A topoisomerase II-dependent G2 cycle checkpoint in mammalian cells/. *Nature* **372**, 467–470 (1994).
24. E. Piskadlo, A. Tavares, R. A. Oliveira, Metaphase chromosome structure is dynamically maintained by condensin I-directed DNA (de)catenation. *eLife* **6**, e26120 (2017).
25. J. Roca, R. Ishida, J. M. Berger, T. Andoh, J. C. Wang, Antitumor bisdioxopiperazines inhibit yeast DNA topoisomerase II by trapping the enzyme in the form of a closed protein clamp. *Proc. Natl. Acad. Sci. U.S.A.* **91**, 1781–1785 (1994).
26. K. L. Furniss *et al.*, Direct monitoring of the strand passage reaction of DNA topoisomerase II triggers checkpoint activation. *PLoS Genet.* **9**, e1003832 (2013).
27. D. A. Skoufias, F. B. Lacroix, P. R. Andreassen, L. Wilson, R. L. Margolis, Inhibition of DNA decatenation, but not DNA damage, arrests cells at metaphase. *Mol. Cell* **15**, 977–990 (2004).
28. K. Maeshima, U. K. Laemmli, A two-step scaffolding model for mitotic chromosome assembly. *Dev. Cell* **4**, 467–480 (2003).
29. F. Mora-Bermúdez, D. Gerlich, J. Ellenberg, Maximal chromosome compaction occurs by axial shortening in anaphase and depends on Aurora kinase. *Nat. Cell Biol.* **9**, 822–831 (2007).
30. J. F. Marko, E. D. Siggia, Polymer models of meiotic and mitotic chromosomes. *Mol. Biol. Cell* **8**, 2217–2231 (1997).
31. N. Kleckner *et al.*, A mechanical basis for chromosome function. *Proc. Natl. Acad. Sci. U.S.A.* **101**, 12592–12597 (2004).
32. J. H. Gibcus *et al.*, A pathway for mitotic chromosome formation. *Science* **359**, eaao6135 (2018).
33. K. Maeshima, S. Iida, S. Tamura, Physical nature of chromatin in the nucleus. *Cold Spring Harb. Perspect. Biol.* **13**, a040675 (2021).
34. S. Hauf, Y. Watanabe, Kinetochore orientation in mitosis and meiosis. *Cell* **119**, 317–327 (2004).
35. R. A. Oliveira, R. S. Hamilton, A. Pauli, I. Davis, K. Nasmyth, Cohesin cleavage and Cdk inhibition trigger formation of daughter nuclei. *Nat. Cell Biol.* **12**, 185–192 (2010).
36. J. Liu, D. M. Czajkowsky, S. Liang, Z. Shao, Cell cycle-dependent nucleosome occupancy at cohesin binding sites in yeast chromosomes. *Genomics* **91**, 274–280 (2008).
37. T. J. Wendorff, B. H. Schmidt, P. Heslop, C. A. Austin, J. M. Berger, The structure of DNA-bound human topoisomerase II alpha: Conformational mechanisms for coordinating inter-subunit interactions with DNA cleavage. *J. Mol. Biol.* **424**, 109–124 (2012).